

Volume change behaviour of saturated sand under thermal cycles

Journal: Géotechnique Letters

Type of paper: Technical paper

Author: C.W.W. Ng, S.H. Wang* & C. Zhou

*Corresponding author

Information of the authors

Crown author: Dr C.W.W. Ng

Chair professor, Department of Civil and Environmental Engineering, the Hong Kong University of Science and Technology, Clear Water Bay, Kowloon, Hong Kong.

Email: cecwwng@ust.hk

Corresponding author: Mr. S.H. Wang

Research student, Department of Civil and Environmental Engineering, the Hong Kong University of Science and Technology, Clear Water Bay, Kowloon, Hong Kong.

Email: swangbf@connect.ust.hk

Co-author: Dr C. Zhou

Visiting assistant professor, Department of Civil and Environmental Engineering, the Hong Kong University of Science and Technology, Clear Water Bay, Kowloon, Hong Kong.

Email: czhou@connect.ust.hk

Introduction

In geo-energy and geo-environmental engineering, soils in many earth structures, including energy piles and landfill covers, are subjected to heating and cooling cycles. The thermally induced soil volume changes can have dramatic consequences for the serviceability of these structures. Up to date, the behaviour of clay and silt under thermal loads has been widely studied (Campanella and Mitchell, 1968; Cui et al. 2000; Abuel-Naga et al. 2007; Vega and McCartney, 2014; Ng and Zhou, 2014; Zhou et al., 2015). Relatively little research has been reported on the volume changes of sand under thermal loads, although sand is always encountered in the above earth structures.

Through temperature-controlled oedometer tests, Kosar (1983) studied heating-induced volume changes of a dry silica sand. Soil axial strain, which was assumed to be equal to volumetric strain, was measured using a linear variable differential transformer (LVDT). When heated from 20 to 50°C at vertical effective stress of 50 kPa, dense and loose sand specimens showed volumetric contractions of approximately 0.06% and 0.4% respectively. Further heating above 50°C induced both specimens to expand volumetrically. It should be pointed out that the oedometer ring, which was made of steel with a linear thermal expansion coefficient of 1.6×10^{-5} per °C (approximately two times that of sand particles (Di Donna and Laloui, 2015)), expanded under heating. This significant expansion would induce additional axial settlement of soil specimens, and therefore the measured axial deformation may not represent the intrinsic thermo-mechanical soil behaviour. Furthermore, only a single heating process was

considered in Kosar's tests. Chen et al. (2006) packed another type of granular material (glass beads) in a plastic cylindrical container and applied thermal cycles under zero external load in the temperature range of 22 to 41°C. The granular packing showed progressive settlement (up to 3.5% axial strain) over 40 thermal cycles. Similar to Kosar's study, in Chen et al.'s study, the boundary condition of the granular packing changed under thermal cycles due to the thermally induced strain of the plastic container. Without eliminating the influence of changes in boundary conditions, the intrinsic volume changes of granular materials under thermal loads cannot be fully revealed. Another limitation of the above two studies is that stress effects were not considered.

In this study, using a temperature-controlled triaxial apparatus, saturated Toyoura sand with different relative densities (from 21% to 90%) and confining stresses (50 and 200 kPa) was firstly isotopically compressed. Then, volume changes during two cycles of heating and cooling (temperatures from 23 to 50°C) was investigated. Unlike in previous oedometer tests, the effects of changes in boundary conditions were eliminated by using the triaxial apparatus.

Test program

To investigate the thermally induced volume changes of sand, three series of tests were carried out on Toyoura sand, the basic properties of which were reported by Verdugo and Ishihara (1996). The objective of the first series was to study heating-induced soil volume change at the same stress level (mean effective stress, $p' = 200$ kPa) but different initial densities (relative density, $D_r = 21\%$, 70% and 90%). In the second series, a specimen (D20S50H) with initial D_r

of 21% was heated at p' of 50 kPa. By comparing the behavior of D20S50H with that of specimen D20S200H in the first test series, effects of stress on the thermally induced volume change were analyzed. Finally, the third series was designed to study soil volume change under heating and cooling cycles with different initial densities ($D_r = 26\%$ and 70%). Details of the test programs are summarized in Table 1.

It should be pointed out that the range of soil stress and density in this study is chosen with reference to energy pile. Given the pre-designed stress and density, the state of all specimens before heating is on the dry side of the critical state line. The state parameter, which is defined by Been and Jefferies (1985) as the difference between the current and critical void ratio at the same mean effective stress, is calculated and summarized in Table 1. The value of state parameter is negative for all specimens, ranging from -0.282 to -0.012. To highlight the differences between soil specimens, in this paper, the soil state is defined by relative density for simplicity. Specimens with an initial relative density of 21%, 70% and 90% are classified as loose, medium dense and dense specimens, respectively (Budhu, 2015).

Test apparatus

Figure 1(a) shows a schematic diagram of the apparatus used in this study. The apparatus was modified from a computer-controlled Global Digital Systems (GDS) triaxial apparatus by adding a temperature control system. The temperature control system consisted of a water bath, a heating/cooling unit, a circulating pump, a spiral metal tube, a thermostat and three thermocouples (T1, T2 and T3). During the test, water inside the water bath was heated/cooled

by the heating/cooling unit and then circulated around the sample with the help of the circulating pump and spiral metal tube. A soil specimen was heated/cooled through heat exchange with the circulating water. To maintain the soil temperature at a given value, T3 was placed at a distance of approximately 5 mm from the specimen. This thermocouple gave feedback to the thermostat, which in turn adjusted the power of the heating/cooling unit until thermal equilibrium was reached. Furthermore, to check the uniformity of soil temperature, T1 and T2 were used to measure soil temperature at the top and bottom boundaries. When temperature equilibrated near the target value, the difference between T1 and T2 measurements was less than 0.4°C, and temperature fluctuation was below 0.2°C, suggesting that stable and uniform soil temperatures were achieved.

According to Cekerevac et al. (2005), the thermally induced volumetric strain of soil skeleton (assembly of soil particles) is calculated using the following equation:

$$\varepsilon_v(T) = (\Delta V_{dr}(T) - \Delta V_{de}(T) - \Delta V_w(T) - \Delta V_s(T) - \mu t)/V \quad (1)$$

where $\Delta V_{dr}(T)$ is the volume of water expelled out from the specimen measured by the GDS pressure/volume controller; $\Delta V_{de}(T)$ is the thermal expansion of the water drainage system; $\Delta V_w(T)$ and $\Delta V_s(T)$ are the thermal expansions of pore water and of soil particles, respectively; μ/V is the water diffusion rate through the membrane and tube connections at a given pressure and temperature; t is the duration of thermal loading; and V is volume of the specimen prior to thermal loading. It should be noted that during non-isothermal tests, the soil particles and pore water in soil specimens experience thermal expansion and contraction under heating and

cooling cycles. As illustrated by Campanella and Mitchell (1968), apart from volumetric strain of soil skeleton $\varepsilon_v(T)$, the thermal volume changes of pore water and soil particles would induce water exchange between soil specimen and the GDS pressure/volume controller. To calculate $\varepsilon_v(T)$ from measured $\Delta V_{dr}(T)$, the third and fourth terms on the right-hand side of equation (1) are included to consider thermal volume change of soil particles and pore water respectively.

In this study, thermally induced volume change of soil specimen is determined by monitoring the volume of water drained from the specimen using a GDS pressure/volume controller. To account for the thermal expansion and contraction of the water drainage system (i.e., drainage tube, porous stone and water filling them) during heating and cooling cycles, the calibration procedures recommended by Cekerevac et al. (2005) are adopted. The relationship between applied temperature and measured volume change of drainage system is shown in Figure 1(b). It can be seen that under heating and cooling cycle, the expansion of the drainage system exhibits slight hysteresis. The calibration curve in this figure is used to determine $\Delta V_{de}(T)$ in equation (1) for correcting measured soil volume changes due to the thermal expansion and contraction of the drainage system. In addition, it should be pointed out that at constant confining pressure condition, the cell wall and cell fluid are free to expand and contract under heating and cooling cycles. The influence of their thermal expansion and contraction on soil stress state and volume change should be negligible. On the other hand, during the test, the rate of thermal loading is slow (i.e., about 1°C per hour). A drainage line of about 1.5 m is used to

connect a soil specimen and the GDS pressure/volume controller. With such a slow thermal loading rate and a long drainage line, it may be reasonable to expect that the temperature of the water drained out from the specimen should change to the room temperature before entering the GDS controller. Consequently, thermal effects on the GDS controller should be very negligible.

Great cares are taken to improve the accuracy of $\varepsilon_v(T)$ measurements in this study. In particular, $\Delta V_{dr}(T)$ was measured by a GDS controller filled with de-aired water in a room with daily temperature fluctuation less than 1 °C so that the oscillation of volume measurement can be minimized. $\Delta V_{dc}(T)$ was well calibrated, as shown in Figure 1(b). From the thermal expansion coefficients of water and sand particle reported by Baldi et al. (1988) and Agar (1984) respectively, $\Delta V_w(T)$ and $\Delta V_s(T)$ were calculated and summarised in Table 3. To minimize water diffusion μ , two high temperature resistant neoprene membranes separated by silicon grease and sealed by high temperature resistant O-rings were used in the tests. Moreover, two hose clamps were used to tighten O-rings and high performance epoxy adhesive was used to seal drainage tube connections with top caps. With careful calibrations, the accuracy of $\varepsilon_v(T)$ measurement is estimated to be 0.02%. More details are given in Table 2.

Specimen preparation and test procedures

In this study, soil specimens with a wide range of densities ($D_r = 21\% - 90\%$) were prepared using the air pluviation method (Vaid and Negussey, 1988). After preparation, the soil specimens were set up in the triaxial apparatus and saturated using the method suggested by

Rad and Wayne Clough (1984) with B-values larger than 0.95.

Figure 2 shows the thermo-mechanical path of specimens after saturation. The specimens were first isotopically compressed to predefined stresses for consolidation ($A \rightarrow D$, $B \rightarrow E$, $C \rightarrow F$, $C \rightarrow G$, $B \rightarrow E$ and $C \rightarrow F$ for tests D90S200H, D70S200H, D20S200H, D20S50H, D70S200TC and D20S200TC, respectively). After consolidation, specimens in the first two series were heated from 23 to 50°C in steps under drained conditions ($D \rightarrow D_1$, $E \rightarrow E_1$, $F \rightarrow F_1$, and $G \rightarrow G_1$ for tests D90S200H, D70S200H, D20S200H and D20S50H, respectively), while specimens in the third series were subjected to two thermal cycles ($E \rightarrow E_1 \rightarrow E \rightarrow E_1 \rightarrow E$ and $F \rightarrow F_1 \rightarrow F \rightarrow F_1 \rightarrow F$ for tests D70S200TC and D20S200TC, respectively).

During the above procedures, the change in excess pore water pressure was less than 2 kPa. The volume change of soil specimens was measured using an advanced GDS pressure/volume controller, which is also used for the control of back pressure in a soil specimen. Figure 3 shows the raw time series data of average soil temperature and volume of water expelled from soil specimen entering the GDS pressure/volume controller in a typical test (D70S200TC). It is clear that the volume of water entering the GDS pressure/volume controller increased under heating but decreased under cooling. For a given temperature increment of 5°C, soil temperature and the measured water volume reach an equilibrium state within 4 hours. At the thermal equilibrium state, the reading of volume measurements shows an oscillation of about 10 mm³, which corresponds to an experimental error of about 0.01%. Based on the measured raw time series data of temperature change and water drained out from the specimen, thermally

induced soil volume change of the soil specimen can be calculated using equation (1). Based on the measured raw time series data of temperature change and water drained out from the specimen (see Figure 3), thermally induced soil volume change of the soil specimen can be calculated using equation (1). The calculated value of each term in equation (1) is summarised in Table 3 for a typical test (D70S200TC). For all other tests in this study, results are processed in similar approach.

Interpretations of experimental results

Heating-induced volume change at different densities

Figure 4 shows the volume change behavior of saturated sand under heating obtained from the first series. For specimens subjected to thermal cycles (D20S200TC and D70S200TC in series 3), the results from the first stage of heating are also included for comparison. As the temperature rose from 23 to 35°C during the first thermal cycle, loose and medium dense specimens showed contractive volumetric strains of approximately 0.15% and 0.05% respectively. These measurements are larger than the achievable accuracy of measurement (i.e., 0.02%). Both specimens exhibited an expansive volumetric strain of approximately 0.05% as the temperature increased further from 35 to 50°C. Two tests were performed for a given density. The almost identical results demonstrate good repeatability of the tests. On the other hand, for the dense specimen, only expansion was observed as the temperature increased from 23 to 50°C.

The observed thermo-mechanical behaviour of sand may be explained from a

microstructure point of view. Through discrete element method (DEM) simulations, Vargas and McCarthy (2007) found that even under constant confining stress, the thermal expansion of sand particles may trigger particle rearrangements and induce plastic volumetric contraction inside the specimen, which would stiffen the soil skeleton. In addition, as shown in Figure 4, the medium dense specimen shows similar response as that of the loose specimen qualitatively. The former, however, shows smaller volume contractions than that of the latter. The similarity between medium dense and loose specimens is probably because they both have some unstable voids (Sitharam, 2003), which could be destroyed by heating-induced particle rearrangements, resulting in contraction during heating. On the contrary, the dense sand specimen behaves differently from the two looser specimens due to its stable compacted structure. Given a more stable structure, the response of dense specimens under heating is essentially elastic (with minimum particle rearrangement), the observed volumetric expansion should mainly come from the thermal expansion of individual sand particle.

The test results of Kosar (1983) (see the Introduction) and the current study show at least two major differences. Firstly, the dense specimens contracted slightly under heating in Kosar's test but expanded in the current study. Secondly, at a given density and stress condition, the thermal contraction measured by Kosar was up to three times larger than that observed in this study. As stated in the introduction, Kosar's tests were carried out in an odometer ring, which was made of steel with a linear thermal expansion coefficient of approximately two times that of sand particles (Di Donna and Laloui, 2015). It is reasonable to expect that under heating, the

oedometer ring would expand more than that of sand and hence induced additional settlement of the specimen. Furthermore, by testing glass-bead packing in cylindrical containers, Chen (2008) found that the measured settlement of the specimen was larger when the thermal expansion coefficient of the container was larger. The above findings well illustrate that thermal expansion of oedometer ring would induce an additional soil settlement during heating. The measurements from the current study represent the intrinsic soil volume change induced by thermal loads.

As shown in Figure 4 that when temperature increases from 23 to 50°C, the maximum contractive volumetric strain of medium dense ($D_r = 70\%$) and loose ($D_r = 21\%$) Toyoura sand specimens under constant isotropic stress of 200 kPa are about 0.05% and 0.15%, respectively. Given the same temperature increase, the thermal volume change for sand measured in this study is about 10 times smaller than that of clay (about 1% for normally consolidated clay (Cui et al., 2000)). To further understand the measured thermally induced volume changes, the compressibility of sand under isotropic compression stress conditions measured by Li (2002) is shown in Figure 5(a). It can be seen that the sand specimens show a nonlinear stress-strain behaviour with a higher compressibility at higher stress level. When the confining stress increases from 200 to 300 kPa, the medium dense ($D_r = 52\%$) and loose ($D_r = 5\%$) specimens show a volumetric strain of about 0.08% and 0.19%, respectively. Therefore, for medium dense and loose sand specimens tested in this study, the amount of thermally induced contraction is comparable to that induced by an incremental mechanical loading of 100 kPa (from 200 kPa to

300 kPa).

On the other hand, the measured thermally induced volume changes are relatively small. It would be interesting to see how far these volume contractions are outside the elastic region on the stress-strain curves. Figure 5(b) shows the measured relationship between shear modulus and strain for Toyoura sand, determined through resonant column and torsional shear tests. Different relative densities (D_r) and confining pressure (p') were considered. It is clear that shear modulus decrease significantly with an increasing strain. When the shear strain exceeds a threshold value of about 0.01%, elasto-plastic behaviour is evident. In this study, the thermally induced contraction for loose specimen is about 0.15%, which is much larger than this threshold strain. It is thus reasonable to deduce that the thermally induced volume strains are already far outside the elastic region on the stress-strain curves for Toyoura sand.

Heating-induced volume change at different stresses

Figure 6 shows the heating-induced volume change of sand at the same density ($D_r = 21\%$) but different stresses ($p' = 50$ and 200 kPa) obtained from the second series. At both stress conditions, the soil responded to heating by first contracting and then expanding. At a quantitative level, heating clearly induced larger strains at higher stress, with 0.15% and 0.07% volumetric contraction at effective stress 200kPa and 50kPa respectively. The observed stress effects can be explained by the state dependency of soil behavior that at a given relative density, a sand specimen at a higher stress behaves like looser sand, which has larger contractive volumetric strain under heating (see Figure 4). Consequently, larger volumetric contraction is

observed when sand is under higher stress.

Volume change during heating and cooling cycles

Figure 7 shows the volume change of loose and medium dense specimens during two thermal cycles obtained from the third series. During the first stage of heating, as reported above, both the loose and medium dense specimens contracted initially before expanding. During the subsequent cooling stage, both specimens contracted with similar magnitude. During the second thermal cycle, both specimens expanded under heating and contracted under cooling. The observed significant cyclic effects are likely because that due to the measured irreversible contraction induced by the first cycle of heating and cooling, soil response becomes stiffer during the second thermal cycle. Given a stiffer soil skeleton, the thermo-mechanical soil behaviour during the second thermal cycles could be essentially elastic during thermal loading within same temperature range.

It should be noted that the observed volume change behaviour of sand under thermal loads cannot be explained by existing thermo-mechanical constitutive models, in which they generally assume that the thermally induced soil volume change is mainly governed by stress history only (e.g., Hueckel and Borsetto, 1990; Cui et al. 2000; Laloui and François, 2009), and typically predict contractive and expansive responses for NC (loose) and highly OC (dense) specimens, respectively. Slightly OC (medium dense) specimen is predicted to firstly expand and then contract.

Conclusions

As soil temperature rose from 23 to 35°C during the first stage of heating, loose and medium dense specimens at mean effective stress of 200 kPa showed contractive volumetric strains of approximately 0.15% and 0.05% respectively. The observed contraction is likely because the thermal expansion of soil particles adjusted soil force chains, inducing plastic contraction and soil hardening. Both specimens showed expansive strain of approximately 0.05% as the temperature increased further from 35 to 50°C. On the contrary, for dense specimen with a more stable structure, only expansion was observed during heating from 23 to 50°C with a volumetric strain of approximately 0.1%. During the second thermal cycle, the responses of specimens with different densities were almost reversible with heating expansion and cooling contraction.

Apart from density, the thermally induced soil volume change was also affected by stress. For loose sand at a given density, when soil temperature was increases from 23 to 50°C, an expansive volumetric strain of -0.02% and a contractive volumetric strain of 0.1% were observed at mean effective stresses of 50 and 200 kPa, respectively.

Acknowledgements

The authors would like to acknowledge the financial support provided by the Research Grants Council (RGC) of HKSAR (GRF 617213, 16209415 and M-HKUST603/13 and SRFDP 20130094140001), the National Natural Science Foundation of China (grant no.s 51378178 and 51509041) and the HKUST (grant no. FP204).

References

- Abuel-Naga, H. M., Bergado, D. T. & Bouazza, A. (2007). Thermally induced volume change and excess pore water pressure of soft Bangkok clay. *Engineering Geology*, 89(1), 144-154.
- Baldi, G., Hueckel, T. & Pellegrini, R. (1988). Thermal volume changes of the mineral-water system in low-porosity clay soils. *Canadian Geotechnical Journal*, 25(4), 807-825.
- Been, K. and Jefferies, M.G. (1985). A state parameter for sands. *Géotechnique*, 35(2), 99–112.
- Budhu, M. (2015). *Soil Mechanics Fundamentals*. John Wiley & Sons.
- Campanella, R.G. & Mitchell, J.K. (1968). Influence of the temperature variations on soil behaviour. *J. Soil Mech. Found. Eng. Div., ASCE* 94 (SM3), 709–734.
- Cekerevac, C., Laloui, L. & Vulliet, L. (2005). A novel triaxial apparatus for thermo-mechanical testing of soils. *Geotechnical Testing Journal, ASTM*, 28(2), 161-170.
- Chen, K., Cole, J., Conger, C., Draskovic, J., Lohr, M., Klein, K. & Schiffer, P. (2006). Granular materials: Packing grains by thermal cycling. *Nature*, 442(7100), 257-257.
- Cui, Y. J., Sultan, N. & Delage, P. (2000). A thermomechanical model for saturated clays. *Canadian Geotechnical Journal*, 37(3), 607-620.
- Di Donna, A. & Laloui, L. (2015). Response of soil subjected to thermal cyclic loading: experimental and constitutive study. *Engineering Geology*, 190, 65-76.
- Donaghe, R. T., Chaney, R. C. & Silver, M. L. (1988). Influence of Filter Paper and Leakage on Triaxial Testing. In *Advanced triaxial testing of soil and rock*, ASTM STP 977, pp. 189-201. Philadelphia, PA: American Society for Testing and Materials.
- Haug, M. D., Buettner, W. G. & Wong, L. C. (1994). Impact of leakage on precision in low gradient flexible wall permeability testing. *ASTM Special Technical Publication*, 1142, 390-390.
- Hossain, D. (1995). Leakage control in long-duration testing of triaxial specimens. *Journal of Geotechnical Engineering, ASCE*, 121(11), 810-813.
- Hueckel, T., & Borsetto, M. (1990). Thermoplasticity of saturated soils and shales: constitutive equations. *Journal of Geotechnical Engineering, ASCE*, 116(12), 1765-1777.

- Iwasaki, T., Tatsuoka, F., & Takagi, Y. (1978). Shear moduli of sands under cyclic torsional shear loading. *Soils and foundations*, 18(1), 39-56.
- Kosar, K. M. (1983). The effect of heated foundations on oil sand. M.Sc. thesis, University of Alberta, Edmonton, Alta., 248 p.
- Laloui, L. & François, B. (2009). ACMEG-T: soil thermoplasticity model. *Journal of Engineering Mechanics*, ASCE, 135(9), 932-944.
- Li, X. S. (2002). A sand model with state-dependent dilatancy. *Géotechnique*, 52(3), 173-186.
- Ng, C. W. W. & Zhou, C. (2014). Cyclic behaviour of an unsaturated silt at different suctions and temperatures. *Géotechnique*, 64(9): 709 –720.
- Rad, N. & Wayne Clough, G. (1984). New Procedure for Saturating Sand Specimens. *Journal of Geotechnical Engineering*, ASCE, 110(9), 1205–1218.
- Sitharam, T. G. (2003). Discrete element modelling of cyclic behaviour of granular materials. *Geotechnical & Geological Engineering*, 21(4), 297-329.
- Tanaka, N. (1995). Thermal Elastic Plastic Behavior and Modeling of Saturated Clays, Ph. D. Thesis, The University of Manitoba, Manitoba, Canada.
- Vaid, Y. P. & Negussey, D. (1988). Preparation of reconstituted sand specimens. In *Advanced triaxial testing of soil and rock*, ASTM STP, 977, pp. 405-417.
- Vargas, W. L. & McCarthy, J. J. (2007). Thermal expansion effects and heat conduction in granular materials. *Physical Review E*, 76(4), 041301.
- Vega, A. & McCartney, J.S. (2014). Cyclic heating effects on thermal volume change of silt. *Environmental Geotechnics*, pp. 1-12. <http://dx.doi.org/10.1680/envgeo.13.00022>.
- Verdugo, R. & Ishihara, K. (1996). The steady state of sandy soils. *Soils and Foundations*, 36(2): 81–91.
- Wang, Y. H., Lau, Y. M., & Gao, Y. (2014). Examining the mechanisms of sand creep using DEM simulations. *Granular Matter*, 16(5), 733-750.
- Zhou, C., Xu, J. & Ng, C. W. W. (2015). Effects of temperature and suction on secant shear

modulus of unsaturated soil. *Géotechnique Letters*, 5: 123-128.

List of Tables:

Table 1. Details of experimental program

Table 2. Methods of determining each term in equation (1) and important steps to improve measurement accuracy

Table 3. Data processing procedures to determine thermally induced volume change in a typical test (D70S200TC)

List of Figures:

Figure 1(a). Schematic diagram of a temperature-controlled triaxial apparatus;
(b). Relationship between thermal expansion of water drainage system and temperature change during a heating and cooling cycle (cell pressure = 400 kPa, backpressure = 200 kPa)

Figure 2. Thermo-mechanical path of each specimen

Figure 3. Raw time series data of soil temperature and the volume of water entering the GDS controller during a heating and cooling cycle in a typical test (Test D70S200TC)

Figure 4. Heating-induced volume changes of sand with different densities at 200kPa

Figure 5(a). Isotropic compression curves of Toyoura sand (data from Li, 2002)
(b). Small strain stiffness of Toyoura sand (data from Iwasaki et al. 1978)

Figure 6. Heating-induced volume changes of loose sand under different stresses

Figure 7. Volume changes of sand at 200kPa during thermal cycles

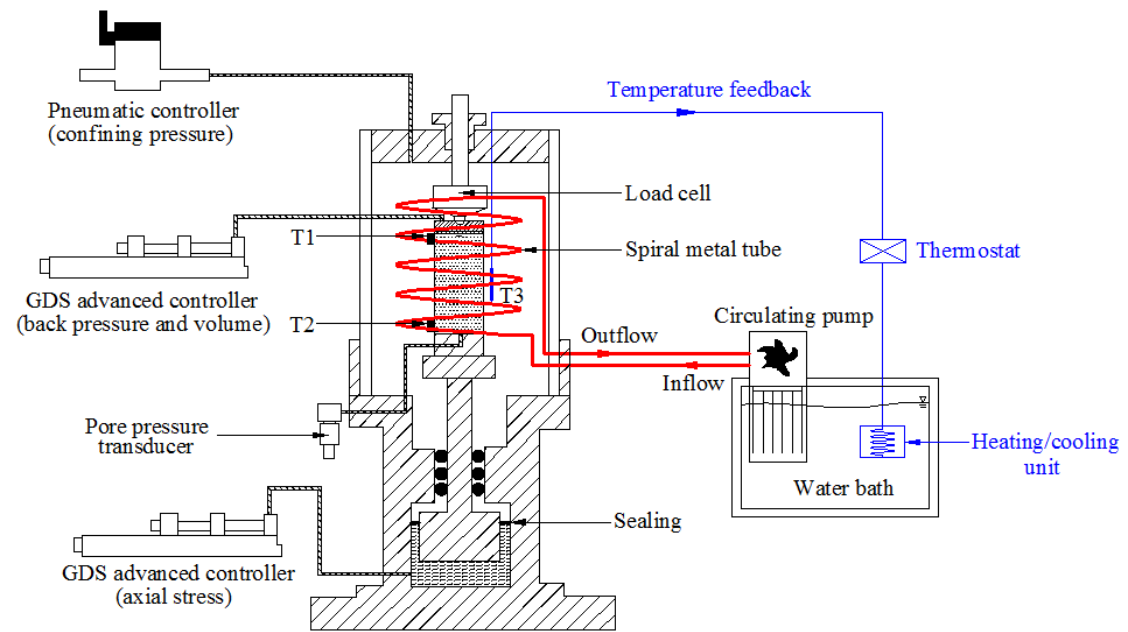


Figure 1(a). Schematic diagram of a temperature-controlled triaxial apparatus

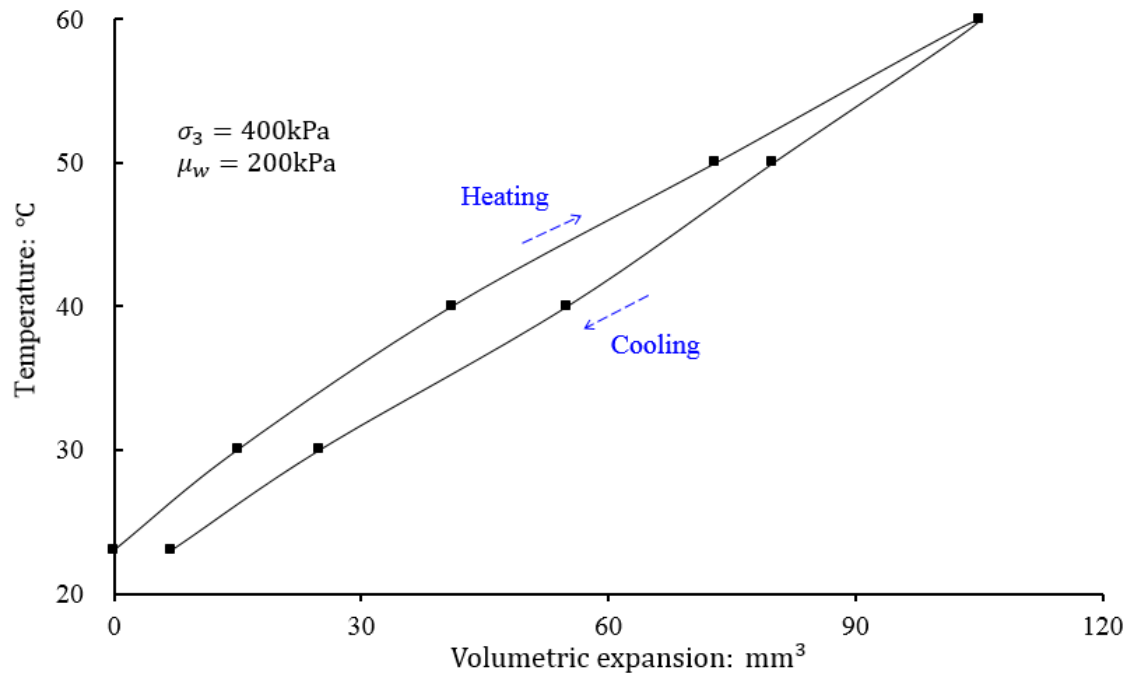
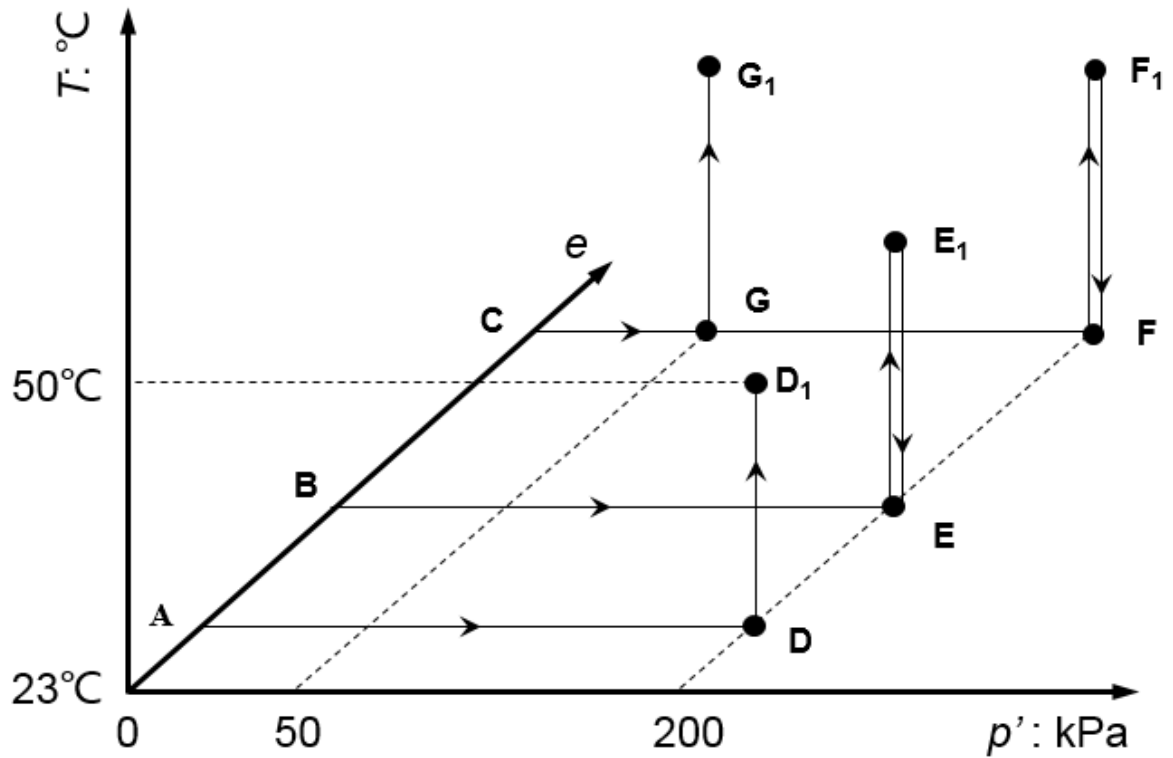


Figure 1(b). Relationship between thermal expansion of water drainage system and temperature change during a heating and cooling cycle (cell pressure = 400 kPa, backpressure = 200 kPa)



Note:

- [1] p' , e and T are the mean effective stress, void ratio and soil temperature, respectively.
- [2] The void ratio of soil specimen would change under mechanical and thermal loads. For simplicity, however, any change of void ratio is not taken into account in this figure.
- [3] Specimens with an initial state of A, B and C are classified as dense, medium dense and loose specimens respectively based on their relative densities (Budhu, 2015).

Figure 2. Thermo-mechanical path of each specimen

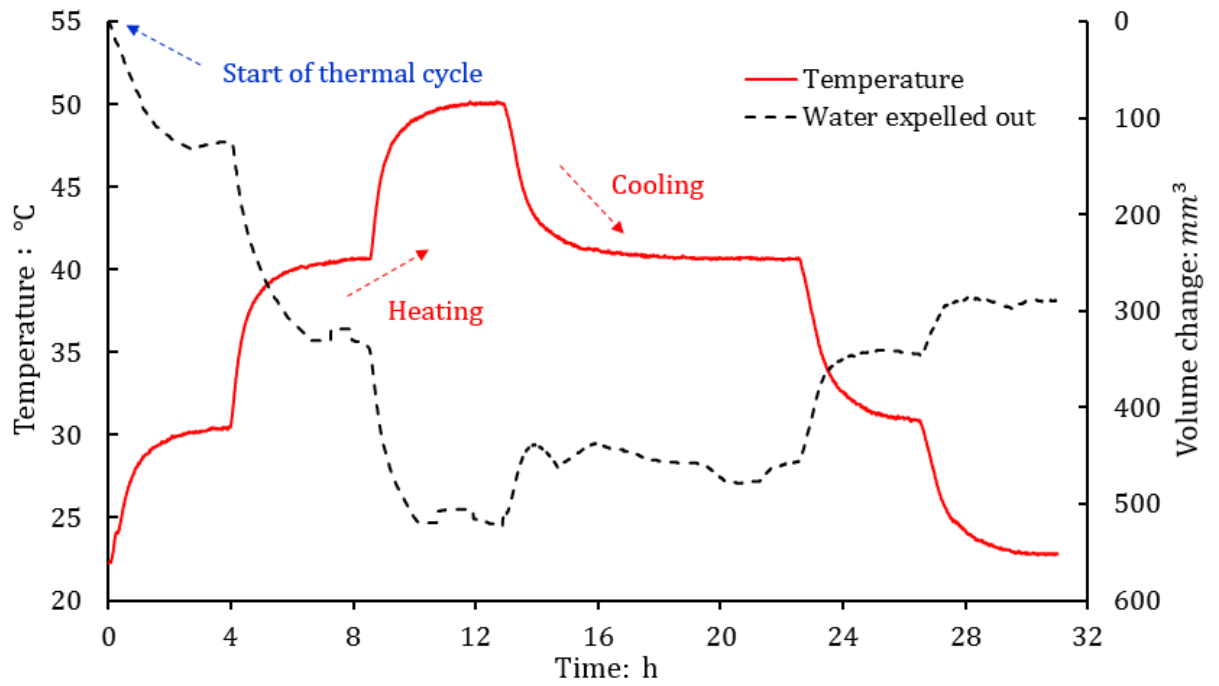


Figure 3. Raw time series data of soil temperature and the volume of water entering the GDS controller during a heating and cooling cycle in a typical test (Test D70S200TC)

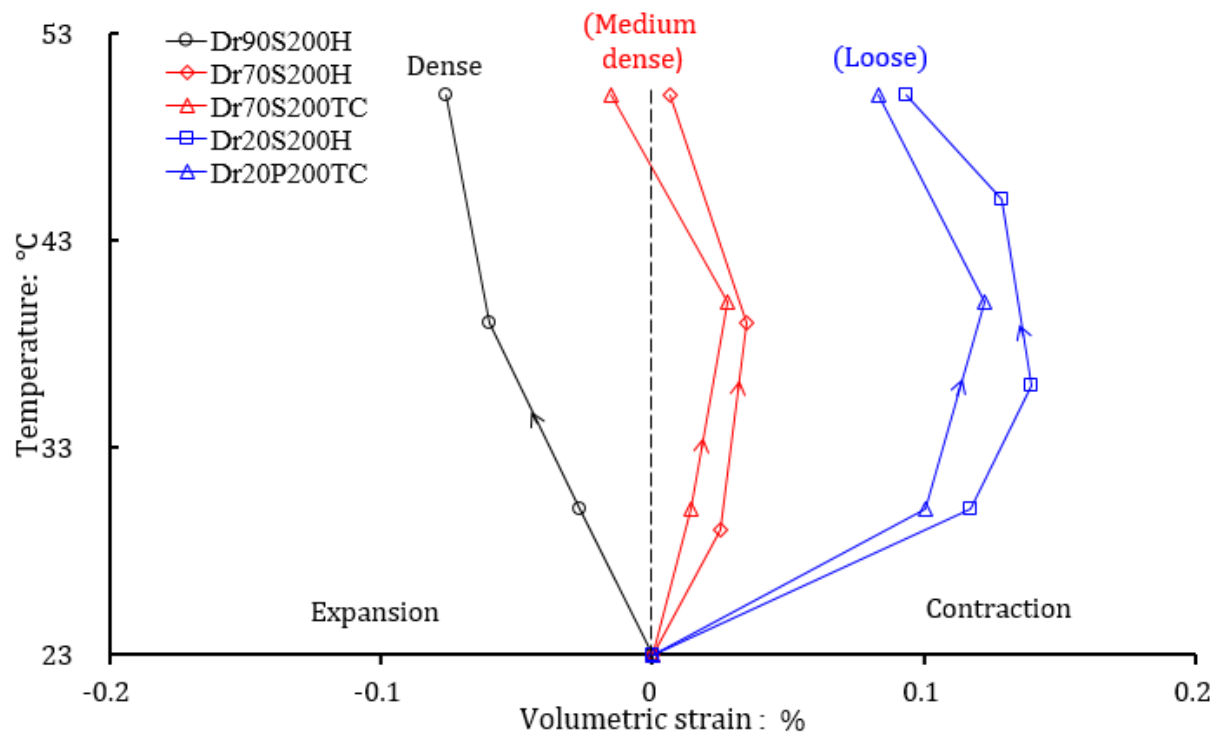


Figure 4. Heating-induced volume changes of sand with different densities at 200kPa

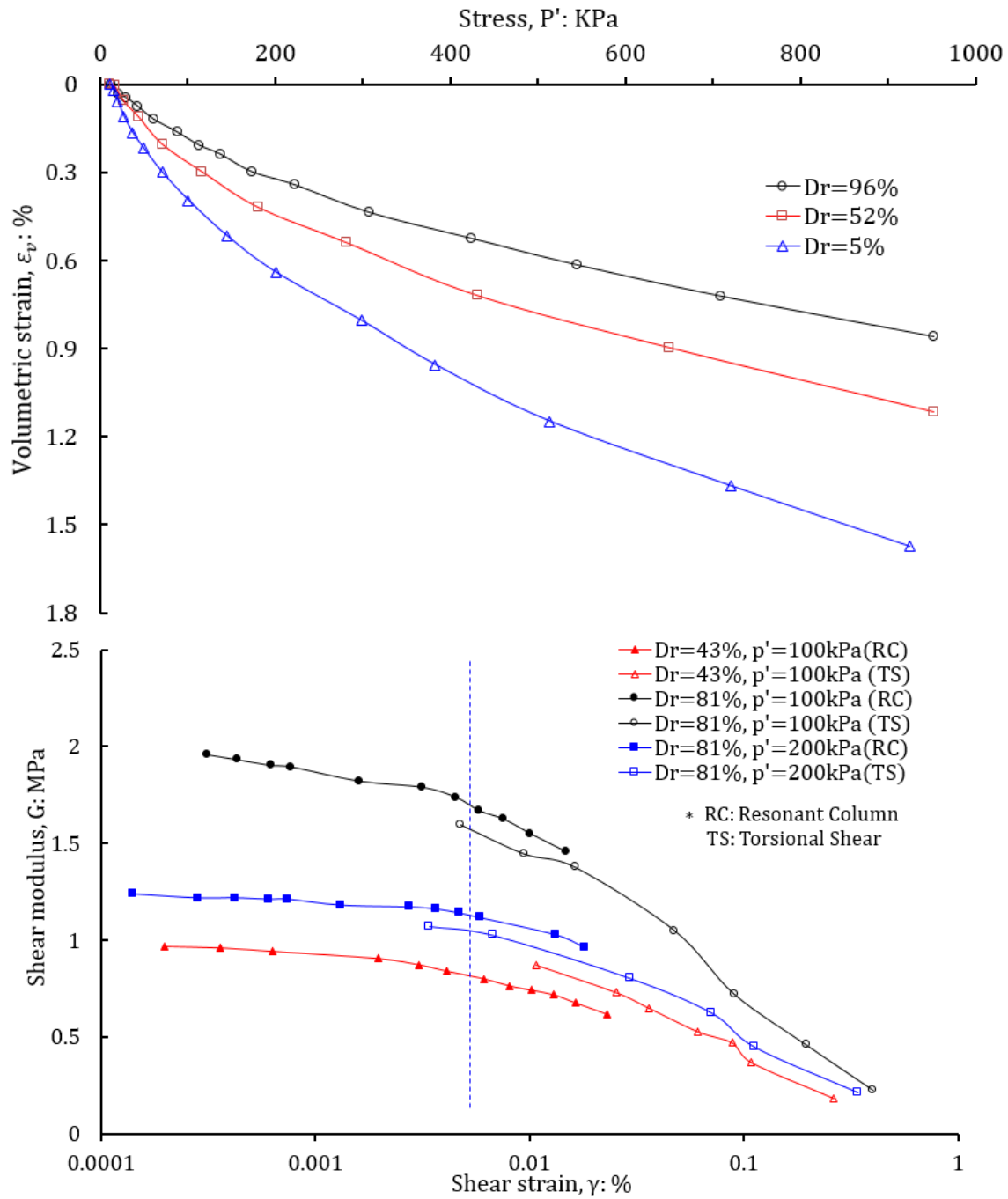


Figure 5(a). Isotropic compression curves of Toyoura sand (data from Li, 2002); (b). Small strain stiffness of Toyoura sand (data from Iwasaki et al. 1978)

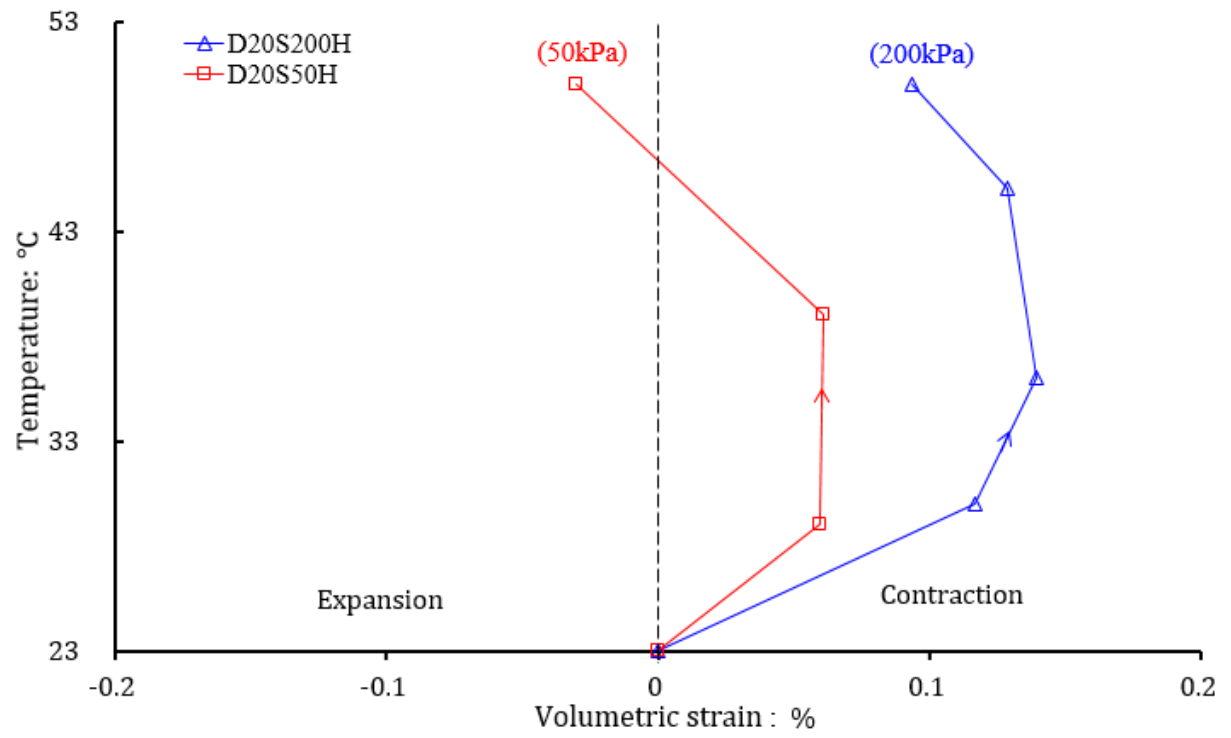


Figure 6. Heating-induced volume changes of loose sand under different stresses

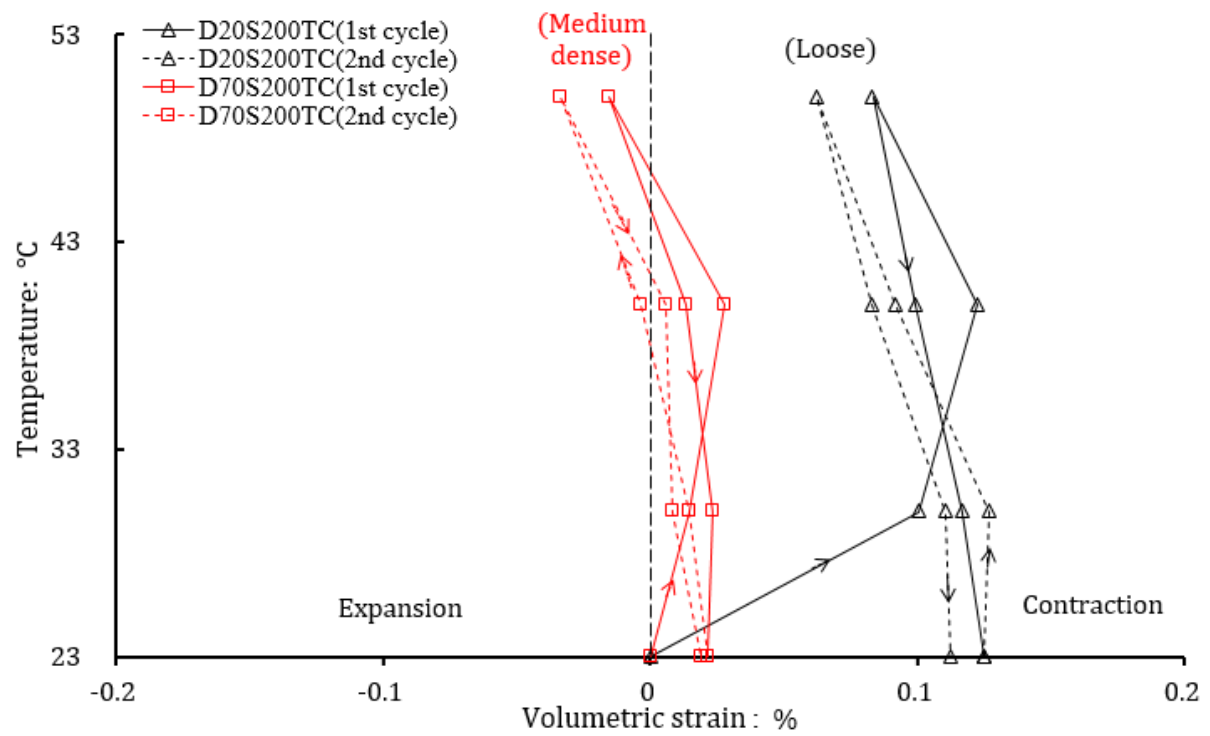


Figure 7. Volume changes of sand at 200kPa during thermal cycles

Table 1. Details of experimental program

Series Number	Specimen Identity	Relative density, D_r^*	Void ratio, e^*	Mean effective stress, p' :	State parameter, ψ^*	Stress path (see Figure 2)
1	D20S200H	21%	0.89	200	-0.012	$C \rightarrow F \rightarrow F_1$
	D70S200H	70%	0.71	200	-0.192	$B \rightarrow E \rightarrow E_1$
	D90S200H	90%	0.62	200	-0.282	$A \rightarrow D \rightarrow D_1$
2	D20S50H	21%	0.90	50	-0.021	$C \rightarrow G \rightarrow G_1$
3	D20S200TC	26%	0.87	200	-0.062	$C \rightarrow F \rightarrow F_1 \rightarrow F \rightarrow F_1 \rightarrow F$
	D70S200TC	70%	0.71	200	-0.212	$B \rightarrow E \rightarrow E_1 \rightarrow E \rightarrow E_1 \rightarrow E$

Note:

* D_r , e , ψ are the values prior to thermal cycle.

Table 2. Methods of determining each term in equation (1) and important steps to improve measurement accuracy

Terms in equation (1)	Determination methods and accuracy improvements
$\Delta V_{dr}(T)$	Measured using a GDS controller (see Figure 1). To improve the accuracy, all tests were carried out in a room with less than $\pm 1^\circ\text{C}$ temperature fluctuation and the GDS controller was filled with de-aired water. The daily fluctuation of volume measurements was less than 0.01% of specimen volume.
$\Delta V_{de}(T)$	Determined by calibrating the thermally induced deformation of the water drainage system at different back pressures, cell pressures and temperatures before the test.
$\Delta V_w(T)$ and $\Delta V_s(T)$	Calculated using the following equations (Baldi et al., 1988; Cekerevac et al., 2005): $\Delta V_w(T) = \alpha_w V_w \Delta T$ and $\Delta V_s(T) = \alpha_s V_s \Delta T$, where α_w and α_s are the thermal expansion coefficients of water and soil particles respectively; V_w and V_s are the volumes of pore water and soil particles respectively; and ΔT is the change in temperature.
μt	Determined by calibrating the water diffusion rate through the membrane (Tanaka, 1995) and tube connections (Haug et al., 1994) at different cell pressures, back pressures and temperatures before the test. To minimize the diffusion rate, two neoprene membranes (working temperatures from -30 to 130°C) separated by silicon grease were used in each test (Hossain, 1995); high temperature resistant O-rings were used to seal membranes; hose clamps were adopted to tighten O-rings (Donaghe et al., 1988); and high performance epoxy adhesive was used to seal drainage tube connections with top caps. The measured average and maximum values of μ were 0.001% and 0.003% of specimen volume per hour, respectively. The average value was used to calculate μt . In this study, the duration of each thermal stage was about 5 hours, so the measurement errors of μt should be less than 0.01% of specimen volume.

Note: Considering that the measurement accuracy of both $\Delta V_{dr}(T)$ and μt is approximately 9 mm^3 (corresponding to 0.01% of specimen volume), the accuracy of the volumetric strain measurement is 0.02%.

Table3. Data processing procedures to determine thermally induced volume change in a typical

test (D70S200TC)

T (°C)	t (h)	$\Delta V_{dr}(T)$ (mm ³)	$\Delta V_{dc}(T)$ (mm ³)	$\Delta V_w(T)/V$ (%)	$\Delta V_s(T)/V$ (%)	$\mu t/V$ (%)	$\varepsilon_v(T)$ (%)
23	0	0	0	0	0	0	0.000
30	4	132	15	0.08	0.003	0.04	0.014
40	8.8	337	41	0.224	0.006	0.088	0.028
50	12.9	527	76	0.399	0.01	0.129	-0.016
40	22.5	464	55	0.233	0.006	0.225	0.014
30	26.5	342	25	0.08	0.003	0.265	0.022
23	31	291	7	0	0	0.31	0.022